Available online at www.sciencedirect.com

ScienceDirect

Procedia Engineering 84 (2014) 770 – 778

Procedia Engineering

www.elsevier.com/locate/procedia

"2014 ISSST", 2014 International Symposium on Safety Science and Technology

Optimization research of hydraulic support in fully mechanized caving face

NIE Wen[a,b,*], CHENG Weimin[a,b], ZHANG Lei[a,b], ZHAO Shuping[a,b], WANG Hao[a,b], ZHU Liang[a,b]

[a]*State Key Laboratory of Mining Disaster Prevention and Contorl Co-founded by Shandong Province and the Ministry of Science and Safety Technology, Shandong University of Science and Technology, Qingdao 266590, Shandong, China*

[b]*College of Mining and Safety Engineering, Shandong University of Science and Technology, Qingdao 266590, Shandong, China*

Abstract

According to the problem that the high concentrations of fully mechanized caving face is difficult to control, the mathematical model of solving two-phase flow of gas and dust particles was built by established the k-ε-Θ-kp equation. Moreover, by basing on Eulerian-Lagrangian model and Eulerian- Eulerian, and using FLUENT software, the diffusion law of dust pollution in full-mechanized caving face was confirmed. The article focuses on existing conditions that the nozzle arrangement of hydraulic support in fully mechanized caving face is flawed so that it can cot to reduce high concentration dust in working face effectively, so we through the theoretical analysis and field test method and the arrangement of equipment at working faces, when spray of forestope is perpendicular to the coal wall, the angle of spraying of truss frames is found to be 45°and the pressure of spraying is 8MPa.Therefore,we take these arguments as the most optimal nozzle arrangement of hydraulic support in fully mechanized caving face. After the research result is applied to the 1303 fully mechanized face of Dongtan Coal Mine, respirable dust fall rate can be high up to 95.8%, dust concentration in working face is reduced effectively, the working condition is mostly improved and the mining is prevented from the danger and low-efficiencies.

Peer-review under responsibility of scientific committee of Beijing Institute of Technology

Keywords: fully mechanized caving face; hydraulic support; nozzle; spray and dust reduction

* Corresponding author. Tel.: +86-18954835917.

E-mail address: sdniewen@163.com

Peer-review under responsibility of scientific committee of Beijing Institute of Technology

doi:10.1016/j.proeng.2014.10.495

1. Instruction

Fully mechanized caving face may product coal at one time which was used to be mined hierarchically for many times，which has advantages of high yield, high efficiency and low consumption. But some problems arise with that such as coal loss, dust and gas management which need solving urgently, especially the high concentration of dust did harm to workers' health and caused a serious threat to the safety production of coal mine. According to the determination, the dust concentration reached 5000mg/m^3[1] when no dust prevention measure is taken. At present, the dust prevention measures of fully mechanized caving face in China are mainly divided into five classes, which are coal water injection, spray dust, ejector dust, dust ventilation and dust control. And the spray dust, which possesses the advantages of economic, convenient and practical, has become the measure that was most widely used in fully mechanized caving face. Hydraulic support spray is the main measure to control the moving frame, dust production of coal drawing, and the important measure to control dust-production by coal cutter[2-5]. Therefore, hydraulic support spray is the most important means of dust-proof of fully mechanized caving face. But the existing research has not yet been nozzle arrangement of fully-mechanized caving hydraulic support a detailed study. But the existing research has not yet been studied in the nozzle arrangement of hydraulic support in fully mechanized caving face, the surface dust, the effect is not good, high dust concentration at the site. As a result, this article has carried on the fully-mechanized caving hydraulic support nozzle arrangement optimization research and the successful application of Dongtan Coal Mine 1303 fully mechanized caving face.

2. An introduction to 1303 fully mechanized caving mining face

1303 fully mechanized caving face is located a lower part of Dongtan coal mine, which length is 239m,it adopted the coal cutting method of trend longwall roof fully mechanized sublevel caving once mining full and daily output is 18351.3 tons. The working face is equipped with ZF8500/21/40YD two-leg shield top-coal caving hydraulic powered support.Hydraulic support installed three groups of spray device: front ground beam spray, spray between frame and coal drawing mouth spray, spray between frame beams before explore decorate 2 nozzle, coal port 1 nozzle spray. Front ground beam spray trapped dust in coal leeward when the fallout, at the same time, it plays the role of wetting of coal wall. Frame between spray is trap dust because of the moving frame or the caving, also plays a guiding romantic and wetting dust on leeward adjacent stent. Coal drawing mouth spray is a trap for moving frame or the caving of dust, it also plays a guiding role for the wind flow.

3. Dust distribution law of the numerical simulation in fully mechanized caving face

3.1. The mathematical model

k-ε-Θ-k_p model is different from two-fluid model, k-ε-Θ-k_p model fixed theory the classic Kinetic theory ,and it disposed of two particle collision dynamics, particle phase stress ,such as particle phase viscosity expression and particle phase pressure expression were deduced, and the close the equations that is suitable to describe particle flow is also derived[6-8].

According to fully mechanized caving face gas-dust two-phase flow are generally under turbulent state, so fluid mechanics model should include the turbulent model equation that gas phase and particle phase are made calculations by reynolds time-averaged[9-11].

Continuity equation of gas phase

$$\frac{\partial(\alpha\rho)_g}{\partial t}+\frac{\partial\left(\alpha\rho\vec{U}_i\right)_g}{\partial x_i}=-\frac{\partial}{\partial x_i}\left[\overline{(\alpha\rho)_g'\vec{U}_{i,g}'}\right] \tag{1}$$

where q is gas phase; α is control body volume fraction of gas phase; $\vec{U}$ is velocity vector, m/s; t is time vector, s; i is an index sign of tensor, i= 1, 2, 3.

Continuous equation of particle density

$$\frac{\partial(\alpha\rho)_p}{\partial t}+\frac{\partial\left(\alpha\rho\vec{U}_i\right)_p}{\partial x_i}=-\frac{\partial}{\partial x_i}\left(\overline{\left(\alpha_p\rho_p\right)'\vec{U}_{i,p}'}\right) \tag{2}$$

Momentum equations of gas phase

$$\frac{\partial\left(\alpha\rho\vec{U}_j\right)_g}{\partial t}+\frac{\partial\left(\alpha\rho\vec{U}_i\vec{U}_j\right)_g}{\partial x_i}=-\alpha_g\frac{\partial P}{\partial x_j}+\alpha_g\rho_g g_j+\frac{\partial\tau_{i,j}}{\partial x_i}+\beta_j\left(\vec{U}_{j,p}-\vec{U}_{j,g}\right)-\frac{\partial}{\partial x_i}\left(\alpha_g\rho_g\overline{\vec{U}'_{i,g}\vec{U}'_{j,p}}\right) \tag{3}$$

where $\tau_{i,j}=\mu_g\left[\left(\frac{\partial\vec{U}_{j,g}}{\partial x_i}+\frac{\partial\vec{U}_{i,g}}{\partial x_j}\right)-\frac{2}{3}\delta_{i,j}\frac{\partial\vec{U}_{k,g}}{\partial x_k}\right]$, β_j is the gas-particle drag coefficient between the components in the *j* direction.

Momentum equations of particles[12, 13]

$$\begin{aligned}&\frac{\partial\left(\alpha\rho\vec{U}_j\right)_p}{\partial t}+\frac{\partial\left(\alpha\rho\vec{U}_i\vec{U}_j\right)_p}{\partial x_i}=-\alpha_p\frac{\partial P}{\partial x_j}+\rho_p g_j+\frac{\partial\Pi_{i,j}}{\partial x_i}+\beta_j\left(\vec{U}_{j,g}-\vec{U}_{j,p}\right)-\frac{\partial}{\partial x_i}\left(\alpha_p\rho_p\overline{\vec{U}'_{j,p}\vec{U}'_{i,p}}\right)\\&-\frac{\partial}{\partial x_i}\left(\vec{U}_{j,p}\overline{\left(\alpha_p\rho_p\right)'\vec{U}'_{i,p}}+\vec{U}_{i,p}\overline{\left(\alpha_p\rho_p\right)'\vec{U}'_{j,p}}\right)\end{aligned} \tag{4}$$

$$\Pi_{i,j}=\bar{\Pi}_{i,j}=-p_p+\left(\xi_p-\frac{2}{3}\mu_p\right)\delta_{i,j}\frac{\partial\vec{U}_{k,p}}{\partial x_k}+\mu_p\left(\frac{\partial\vec{U}_{j,p}}{\partial x_i}+\frac{\partial\vec{U}_{i,p}}{\partial x_j}\right) \tag{5}$$

where p_p is particles phase pressure, $p_p=\alpha_p\rho_p[1+2(1+e)\alpha_p g_0]\Theta$; ξ_p is the whole viscosity of particles phase, $\xi_p=\frac{4}{3}\alpha_p{}^2\rho_p d_p g_0(1+e)\sqrt{\frac{\Theta}{\pi}}$; μ_{p} is the shear viscosity of particles phase, $\mu_p=\frac{2\mu_{p,\mathrm{dil}}}{(1+e)g_0}\left[1+\frac{4}{5}(1+e)g_0\alpha_p\right]^2+\frac{4}{5}\alpha_p{}^2\rho_p d_p g_0(1+e)\sqrt{\frac{\Theta}{\pi}}$, $\mu_{p,\mathrm{dil}}=\frac{5}{96}\rho_p d_p\sqrt{\pi\Theta}$.

Formula (2) to (4), *p* is particles phase; j and k are index notation of tensor, p is pressure, g is acceleration of gravity, and the rest symbols are similar with the significance expression in type (1).

Equation of gas turbulent energy

$$\frac{\partial}{\partial t}\left(\alpha_g\rho_g k\right)+\frac{\partial}{\partial x_j}\left(\alpha_g\rho_g\vec{U}_{j,g}k\right)=\frac{\partial}{\partial x_j}\left(\frac{\mu_e}{\sigma_k}\frac{\partial k}{\partial x_j}\right)+G_k+G_p-\alpha_g\rho_g\varepsilon \tag{6}$$

Equation of gas dissipation rate of turbulent energy

$$\frac{\partial}{\partial t}\left(\alpha_g\rho_g\varepsilon\right)+\frac{\partial}{\partial x_j}\left(\alpha_g\rho_g\vec{U}_{j,g}\varepsilon\right)=\frac{\partial}{\partial x_j}\left(\frac{\mu_e}{\sigma_k}\frac{\partial\varepsilon}{\partial x_j}\right)+\frac{\varepsilon}{k}\left[C_1\left(G_k+G_p\right)-C_2\alpha_g\rho_g\varepsilon\right] \tag{7}$$

where $\mu_e=\mu_g+\mu_{g,t}$, $\mu_{g,t}=C_\mu\alpha_g\rho_g k^2/\varepsilon$, $G_k=\mu_{g,t}\left(\frac{\partial\vec{U}_{i,g}}{\partial x_j}+\frac{\partial\vec{U}_{j,g}}{\partial x_i}\right)\frac{\partial\vec{U}_{i,g}}{\partial x_j}$, $G_p=\frac{2\alpha_p\rho_p}{\tau_p}\left(C_p^p\sqrt{k\left(k_p+\Theta\right)}-k\right)$.

Particle turbulent equation, k_p equation

$$\frac{\partial}{\partial t}\left(\alpha_p\rho_p k_p\right)+\frac{\partial}{\partial x_k}\left(\alpha_p\rho_p\vec{U}_{p,k}k_p\right)=\frac{\partial}{\partial x_k}\left(\frac{\mu_{p,t}}{\sigma_\varepsilon}\frac{\partial k_p}{\partial x_k}\right)+G_{kp}-\alpha_p\rho_p\varepsilon_p+\frac{\partial}{\partial x_k}\left(k_p\frac{\mu_{p,t}}{\sigma_\varepsilon}\frac{\partial\alpha_p\rho_p}{\partial x_k}\right) \tag{8}$$

where $G_{kp}=\mu_{p,t}\left(\frac{\partial\vec{U}_{j,p}}{\partial x_i}+\frac{\partial\vec{U}_{i,p}}{\partial x_j}\right)\frac{\partial\vec{U}_{i,p}}{\partial x_k}$, $\varepsilon_p=\frac{2}{\tau_p}\left(C_p^p\sqrt{kk_p}-k_p\right)$.

The above formula constants of turbulent flow are as shown in Table 1.

Table 1. Constants of turbulent flow model.

C_1	C_2	C_μ	σ_k	σ_ε	σ_p	C_p^p
1.44	1.92	0.09	1.0	1.3	0.7	0.85

Gas-solid two-phase flow fluid mechanics control equations of turbulent gas phase-turbulent particle phase were obtained after combining the formula (1) to formula (8). Noteworthy is, because of the lack of reliable connection, this model overlooked the influence of particle turbulent on temperature equation of particles gas and solid drag force expression[14, 15].

The steady control equations of three-dimensional turbulent two-phase flow in cylindrical coordinates can be expressed as the general form: convection term= diffusion term+ source term[16, 17].

General expression of gas phase control equations

$$\frac{\partial}{\partial x}\left(\alpha_g\rho_g u\varphi\right)+\frac{\partial}{r\partial r}\left(r\alpha_g\rho_g v\varphi\right)+\frac{\partial}{r\partial\theta}\left(\alpha_g\rho_g w\varphi\right)=\frac{\partial}{\partial x}\left(\Gamma_\varphi\frac{\partial\varphi}{\partial x}\right)+\frac{\partial}{r\partial r}\left(r\Gamma_\varphi\frac{\partial\varphi}{\partial r}\right)+\frac{\partial}{r^2\partial\theta}\left(\Gamma_\varphi\frac{\partial\varphi}{\partial\theta}\right)+S_\varphi+S_{\varphi p} \quad (9)$$

Eneral expression of dust phase control equations

$$\frac{\partial}{\partial x}\left(\alpha u_p\varphi_p\right)+\frac{\partial}{r\partial r}\left(r\alpha v_p\varphi_p\right)+\frac{\partial}{r\partial\theta}\left(\alpha w_p\varphi_p\right)=\frac{\partial}{\partial x}\left(\Gamma_{\varphi p}\frac{\partial\varphi_p}{\partial x}\right)+\frac{\partial}{r\partial r}\left(r\Gamma_{\varphi p}\frac{\partial\varphi_p}{\partial r}\right)+\frac{\partial}{r^2\partial\theta}\left(\Gamma_{\varphi p}\frac{\partial\varphi_p}{\partial\theta}\right)+S_{\varphi p}+S_{\varphi pg} \quad (10)$$

3.2. Physical model and Boundary conditions

Equal ratio geometric model of $3_{up}1109$ fully mechanized caving face was built by Gambit soft that is Fluent former processing software. This model is a cuboid area: length×width×height =15.0m×10.0m×3.2m, there are ten hydraulic supports, the hydraulic supports number are 1#-10# from air inlet to air outlet; each hydraulic support width is 1.5m; the height from hydraulic support's upper beam to plate is 3.0m; the distance from coal wall to posterior scraper transport front is 9.5m. The front roller cuts top-coal and the back roller cuts bottom coal along airflow direction; meanwhile, advancing support working procedure at 2# hydraulic support and drawing coal process at 3#, the established model was further mesh divided. The internet size of model mesh was hexahedral and after the division is illustrated in Fig. 1.

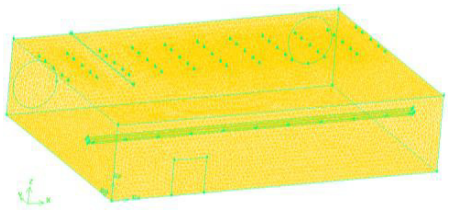

Fig. 1. Physical model after mesh generation.

The boundary condition of the numerical simulation and the parameters of the dust source: inlet speed in fully mechanized caving face is 1.2m/s, dust particle diameter distribution is Rosin-Rammler, the minimal grain diameter is 2.185×10^{-5}m, the maximal grain diameter is 0.85×10^{-6} m, the medium grain diameter is 4.57×10^{-6}m, the distribution parameter is 1.77, dust producing strength is respectively 0.032kg/s, 0.016kg/s, 0.021kg/s when shearer in coal cutting, hydraulic support moving and coal drawing, the tracking times is 3200.

3.3. Simulation result analysis

Gas-dust particle two-phase flow was simulated when shearer in coal cutting, hydraulic support moving and coal drawing at the same. In order to facilitate comparison and analysis, the result of numerical simulation is dust

concentration measure for unity kg/m^3. The dust concentration in all sections of familiar tendency simulation result map is as shown in Fig. 2: Positive direction along *x*: 0, 3m, 6m, 9m, 12m, 15m; *y*: 0, 2.53m, 5.73m, 7.9m, 10m; *z*: 0, 0.8m, 1.6m, 2.4m, 3.2m. The dust concentration of simulation result map at different location is as shown in Fig. 3.

According to the simulation result, primitive dust production of instant high concentration dust group can achieve or exceed 4800mg/m^3 when cutting coal, moving hydraulic support and drawing coal. It is the key of the prevention and control dust in fully mechanized caving face. Dust concentration is as high as 3700mg/m^3 in mainly overlap area of producing dust, especially at 9m down wind side and 1.6m height of breathing zone in dust source of shearer in coal cutting, hydraulic support moving and coal drawing. The dust concentration is still big, changes between 2100-3400mg/m^3 .

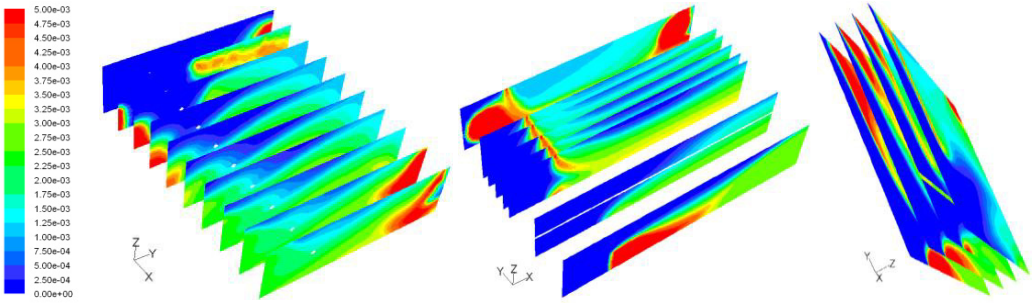

(a) *x* axis (b) *y* axis (c) *z* axis

Fig. 2. The dust concentration of familiar tendency simulation result map along x, y, z axis.

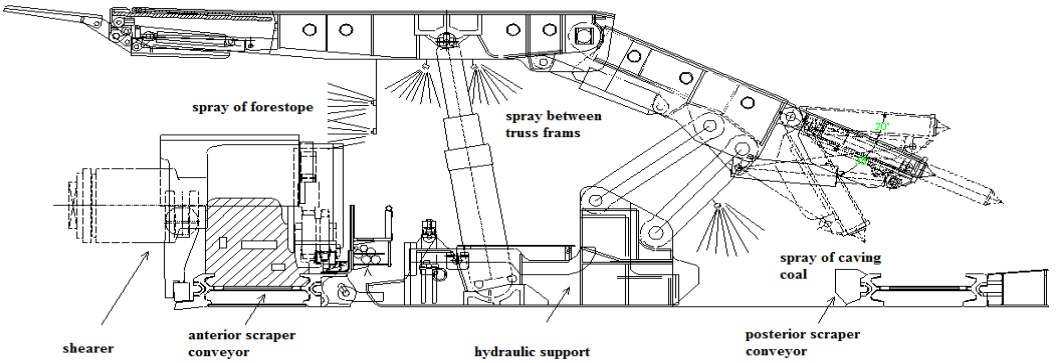

Fig. 3. The current layout of spraying system.

4. The improvement of the nozzle arrangement of hydraulic support

4.1. The improvement of the nozzle arrangement of the spraying of forestope

According to the current layout form of the spraying system of forestope, truss frames and coal drawing as shown in the Fig. 3, the spraying of forestope is not perpendicular to the direction of coal wall. According to the observation, the spraying of forestope has not formed spraying of full section, there is still a huge amount of space near coal wall, which is an important diffusion source of dust. Therefore, the current nozzle arrangement significantly lower the efficiency of dust removal effect. A new way of spraying that the spraying of forestope is perpendicular to the coal wall is designed to solve this. As shown in the Fig. 4, the number of nozzle in different spots of hydraulic support is the same as that in the Fig. 3.

The diffusion angle of nozzle spraying is around 120, and the range of spraying is more than 3.5 meters. The distance between the spraying of forestope and coal wall in the design in the table is 2 meters. In the Fig. 4, the distance between the spraying of forestope and coal wall is 3 meters, and the actually length of pole of spraying of forestope is around 1 meter. The distance between two nozzles and the distance between the upper nozzle and top beam are both 0.5 meter. Fig. 5 and Fig. 6 are simplified figures of the two arrangements of spraying of forestope stated above.

Fig. 4. The effect of forestope is perpendicular to coal wall spray in workface.

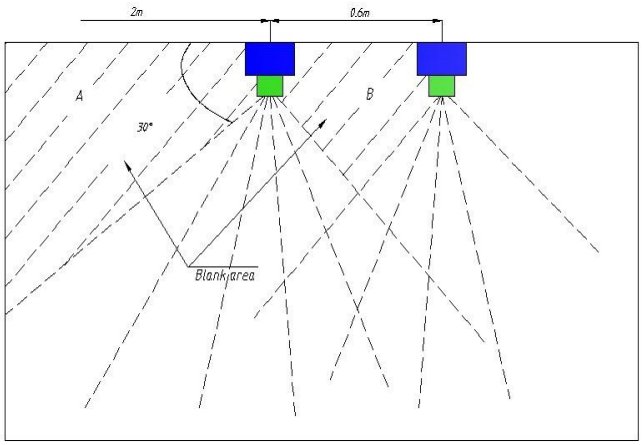

Fig. 5. Forestope is perpendicular to coal drawing spray.

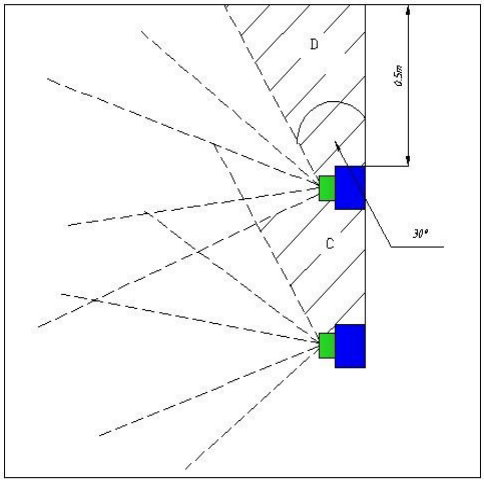

Fig. 6. Forestope is perpendicular to coal wall spray.

According to the Fig. 5 and the Fig. 6, the areas of the space A, B, where the spraying cannot reach, are 1.115 m^2 0.052 m^2 respectively, with a total area of 1.207m^2; however, the areas of the space C, D, where the spraying cannot reach, are 0.036 m^2 0.108 m^2 respectively, with a total area of only 0.108 m^2. Moreover, according to the Fig. 6, the all empty space in C and part of empty space in D are covered by the spraying of truss frames. Therefore, the actually empty space is less than 0.04 m^2, which is greatly smaller than the empty space in Fig. 5. . Therefore, the area covered by the method that the spraying of forestope is perpendicular to coal wall is bigger than that by the

method that the spraying of forestope is perpendicular to coal flow.

When the spraying of forestope is perpendicular to coal wall, for example, the pipe of spraying is designed to be fixed, because the minimal length is around 1 meter, when the roof is not stable and the height of support is low, like 2.8 to 3 meters, and the shearer's height is between 1.8 and 2 meters, the shearer, which moves on the scraper transport, may be blocked when the holding rod of the spraying of forestope falls vertically. An accident that the shearer crushes on the holding rod of nozzle may be easily caused, which will result in the break of the holding rod of nozzle. The break of the holding rod of nozzle will influence the dust removal. Therefore, pole of the spraying of forestope should be designed to be retractable.

4.2. The improvement of the nozzle arrangement of spraying of truss frames

The angle of nozzle of spraying of truss frames is an important factor that influences the dust removal of spraying of truss frames. The angle of nozzle of truss frames in Fig. 3. is 30. In order to enhance the efficiency of spraying dust removal , the angle of nozzle of truss frames should be designed to be adjustable. As shown in Fig. 7, the nozzle of truss frames device is fixed on the top beam by bolts. The angle of nozzle of truss frames can be adjusted by changing the position of the adjuster bolt of chute. Hence, the area covered by the spray can be adjusted.

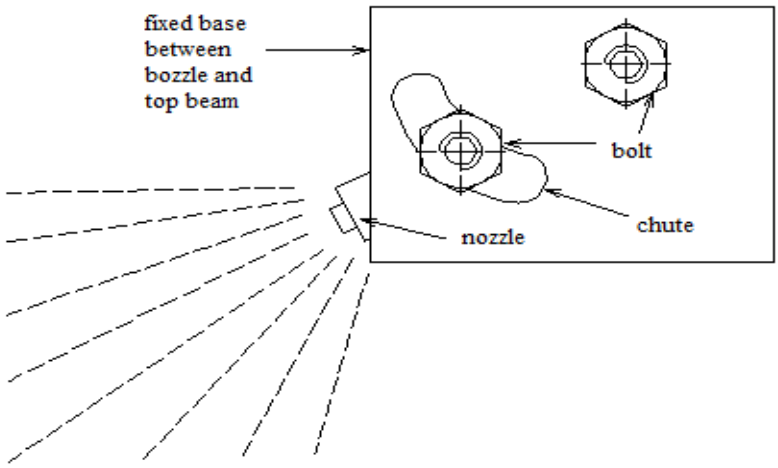

Fig. 7. Spray between frame beams.

The angle of current nozzle of truss frames is 30, and the maximum adjustable angle is 60. Therefore, the best angle can be found by adjusting the angle of nozzle of truss frames and testing the dust removal efficiency. Firstly, test the case where the angle of nozzle of truss frames is 30, then adjust the angle to 45 and 60 and test the efficiency individually. The way to adjust the angle is to loosen the bolts of holding nozzles and turn the nozzle to 45 and 60 along the arc slot of steel entrust.

5. Real case examination

In order to make sure the best setting for the nozzle of hydraulic support in fully mechanized caving face, five tests have been made: the 1303 fully mechanized caving face of Dongtan Coal Mine with only outer and inner mist spray at the coal cutter turned on, with forestope perpendicular to the coal flow, with forestope perpendicular to coal wall (the angles of spraying of truss frames are set to 30, 45 and 60 each time), and the dust concentration of each time is recorded. In addition, in order to determine the most efficient pressure of spraying, each of the five cases

stated above is tested under 6MPa and 8Mpa pressure, and the dust density under each pressure is recorded. The statistics recorded are shown in Table 2.

In Table 2, 1 – stent spraying device is not turned on; 2 - stent spraying device in the setting shown in the Fig. 3, and is turned on; 3 - stent spraying device in the setting shown in the table 2 and is turned on (with stent spraying' s angle turned to 30); 4 - stent spraying device in the setting shown in the Fig. 4, and is turned on (with stent spraying' s angle turned to 45); 5 - stent spraying device in the setting shown in the table 2 and is turned on (with stent spraying' s angle turned to 60); *x*-*y*-1 – the dust removal efficiency under *Y* mPa and number *X* conditions. For example, 2-6-1 means that the efficiency under 6MPa pressure, number 2 condition (stent spraying device in the setting shown in the Fig. 3. and is turned on.

(1) From Table 2, under 6MPa pressure, with the method that the forestope is perpendicular to coal flow direction, the dust density tested in each testing spot is much higher than that with the method that the forestope is perpendicular to the direction of coal wall. Furthermore, with the method that the forestope is perpendicular to the direction of coal wall, different spraying of truss frames' angles affect the efficiency. When the angle is set to be 45, the dust removal effect in procedures of shearer driver, the falling coal of shearer, advancing support, caving coal, and the section of multiple procedures is higher than other situations (where the angles are set to 30 and 60). respirable dust fall rate of the cases stated above are 75.2%,55.4%,94.6%,79.3%,77.0%, respectively; and the total respirable dust fall rate are 64.6%,61.8%,75.6%,64.4%,67.0%, respectively, with an average respirable dust fall rate of 76.3% and an average total dust removal effect of 71.6%.

(2) According to Table 2, with the setting shown in the Fig. 4, under the pressure of 8MPa, the dust density tested in each spot is smaller than that with the same setting but under 6MPa pressure. Moreover, under the pressure of 8MPa, the most efficient method is still the case where the angle of spraying of truss frames is 45. In this case, the respirable dust removal effect is as high as 95.8%, and the total dust removal effect is also higher than that under 6MPa pressure. Therefore, from the statistics analyzed above, the best setting is the case where the angle of spraying of truss frames is 45 and the pressure is 8MPa.

Table 2. The statistics of dust concentration in different spaying conditions.

Number	Pressure	Respiratory Dust Concentration(mg/m^3)					Total Dust Concentration(mg/m^3)				
		Cab	Coal falling	Advancing Support	Caving Coal	Multi-operation	Cab	Coal Falling	Advancing Support	Caving Coal	Multi-operation
1	6MPa	87.5	85.8	188.8	85	55.1	170	191.3	295.1	146.3	133.7
2	6MPa	60	60	80	51.3	43.3	78.3	85.8	258.3	112.7	54
3	6MPa	23.3	41.7	20.5	20	18	67.2	81.5	107.3	63.8	51.6
3	8MPa	18.3	30	16.7	11.7	3.3	60	77.3	46.7	56.7	45.1
4	6MPa	21.7	38.3	10.2	17.6	12.7	60.1	73.1	71.9	52.1	44.1
4	8MPa	11.7	31.6	8	11.2	7.5	52.9	66.3	61.2	48.3	33.8
5	6MPa	30	44.3	50.7	32.3	28.5	95	89	125.8	76.7	48.4
5	8MPa	21.7	26.7	8.3	11.7	5.2	87.5	81.3	63.6	73.3	42.7
Number		Respiratory Dust Dust-laying Rate(%)					Total Dust Dust-laying Rate(%)				
2-6-1		31.4	30.1	57.6	39.6	21.4	53.9	55.1	12.5	23.0	59.6
3-6-1		73.4	51.4	89.1	76.5	67.3	60.5	57.4	63.6	56.4	61.4
3-8-1		79.1	65.0	91.2	86.2	94.0	64.7	59.6	84.2	61.2	66.3
4-6-1		75.2	55.4	94.6	79.3	77.0	64.6	61.8	75.6	64.4	67.0
4-8-1		86.6	63.2	95.8	86.8	86.4	68.9	65.3	79.3	67.0	74.7
5-6-1		65.7	48.4	73.1	62.0	48.3	44.1	53.5	57.4	47.6	63.8
5-8-1		75.2	68.9	95.6	86.2	90.6	48.5	57.5	78.4	49.9	68.1

6. Conclusions

Take all these factors from passages into consideration, we can draw a conclusion that the spraying of the beare has a better dust removal effect when spray of forestope is perpendicular to the coal wall, the angle of spraying of truss frames is found to be 45° and the pressure of spraying is 8MPa.Therefore, we take these arguments as the most optimal nozzle arrangement of hydraulic support in fully mechanized caving face. After the research result is applied

to the 1303 fully mechanized caving face of Dongtan Coal Mine, the dust concentration in working face is reduced effectively, the working condition is mostly improved and the mining is prevented from the danger and low-efficiencies.

Acknowledgments

The authors wish to thank the Key Program of the Coal Joint Funds of the National Natural Science Foundation of China (Grant No. U1261205), the National Natural Science Foundation of China (Grant No. 51074100), the Young Scientists Fund of the National Natural Science Foundation of China (Grant No. 51204103), the Specialized Research Fund for the Doctoral Program of Higher Education of China (Grant No. 20113718110005), the Shandong Provincial Foundation for Development of Science and Technology, China (Grant No. 2013GSF12004).. This work was supported in part by a grant from them.

References

[1] Martin Sommerfeld, "Validation of a stochastic lagrangian modeling approach for inters- particle collisions in homogeneous isotropic turbulence", International Journal of Multiphase Flow, vol. 27, no. 10, pp. 1829-1858, 2001.
[2] Wen Nie, Weimin Cheng, and Gang Zhou, "Experimental study on spray atomized particle size affected by airflow disturbance in heading face", Journal of China University of Mining & Technology, vol. 41, no. 5, pp. 378-383, 2012.
[3] Wen Nie, Caiquan Su, and Weimin Cheng, "Design of water injection technique for high ground pressure low cracking rate seam pressure", Coal Science and Technology, vol. 39, no. 3, pp. 59-62, 2011.
[4] Yajun Li, Hongtao Zheng, and Lin Cai, "Numerical Research on Performance of Swirling Flow Combustor", Journal of Convergence Information Technology, vol. 7, no. 5, pp. 97-105, 2012.
[5] Weimin Cheng, Xiangsheng Liu, and Guoqiang Ruan, "The theory and technology of enclosure dust- laying model in speeded advance of coal road", Journal of China Coal Society, vol. 34, no. 2, pp. 203-207, 2009.
[6] R. Klemens, P. Kosinski, and P. Wolanski, "Numerical study of dust lifting in a channel with vertical obstacles", Journal of Loss Prevention in the Process Industries, vol. 14, no. 6, pp. 469-473, 2001.
[7] Junsheng Guo, Baijian Wu, and Sheji Zhang, "The application of air curtain dust control technology", Safety in Coal Mines, vol. 36, no. 1, pp. 11-13, 2005.
[8] Gang Zhou, Weimin Cheng, and Lianjun. Chen, "Numerical simulation and its application of dust concentration spatial distribution regularities in fully-mechanized caving face", Journal of China Coal Society, vol. 35, no. 12, pp. 2094-2099, 2010.
[9] Panida Songram, Veera Boonjing, "Mining N-Most Interesting Closed Itemsets", Journal of Convergence Information Technology, vol. 7, no. 5, pp. 97-105, 2012.
[10] Haiqiao Wang, Ronghua Liu, and Shiqiang Chen, "Simulation on Flow Field Characteristic of Restricted Wall-attached Jet in Heading Face", Engineering Science, vol. 6, no. 6, pp. 45-49, 2004.